

Photoionization of excited $3d$ states in Na and K: Investigation of the $l \rightarrow l-1$ zeros

Alfred Z. Msezane

Department of Physics, Atlanta University, Atlanta, Georgia 30314

Steven T. Manson

Department of Physics and Astronomy, Georgia State University, Atlanta, Georgia 30303

(Received 24 April 1984)

The photoionization of the excited Na and K $3d$ states have been calculated with use of various numerical and analytic Hartree-Fock wave functions. Particular attention was paid to the zeros in the $3d \rightarrow \epsilon p$ dipole matrix elements and their sensitivity to slight changes in the initial-state wave functions. It was found that only the numerical wave functions were reliable. In addition, it was found that these zeros had virtually no effect on the total subshell cross sections; however, they had a strong influence on the photoelectron angular distributions.

I. INTRODUCTION

Zeros in the dipole matrix element for photoionizing transitions occur often for outer and near-outer shells of ground-state atoms.¹⁻³ These zeros, often called Cooper minima,^{4,5} can occur in the $l \rightarrow l+1$ transition of subshells whose radial wave functions have nodes.¹⁻⁵ More recently, it has been predicted that for excited-state photoionization, zeros can occur in the $l \rightarrow l-1$ transition⁶⁻⁸ and for nodeless subshells.⁷ Furthermore, these zeros were predicted to be a very widespread phenomenon for excited d states of atoms.⁷

Although there is some experimental work on the photoionization of excited states, it is not extensive; the existence of these $l \rightarrow l-1$ zeros has not yet been experimentally verified. Thus it is of interest to have more accurate calculations than the previous central-field model results in order to give experimentalists predictions to test. In addition, it is of interest to determine the sensitivity of these zeros to the details of the wave functions employed in an effort to provide an *a priori* guide to the accuracy of excited-state photoionization calculations.

To this end, we present results for the photoionization of the excited $3d$ state in Na and K. The $3d$ state was chosen because its radial wave function is nodeless and the existence of $l \rightarrow l-1$ zeros is a clear departure from the phenomenology of ground-state photoionization. The alkali-metal atoms Na and K were selected since the simple central-field model predicts both to have a $3d \rightarrow \epsilon p$ zero and the ionization energies are such that they are amenable to laboratory investigation with present laser technology.

The calculations have been performed within the framework of the Hartree-Fock (HF) approximation for both discrete and continuum wave functions. Several different discrete HF methodologies were employed in an effort to determine the sensitivity of the results to slight differences in wave function. These wave functions are discussed in Sec. II along with a brief review of the theory and method of calculation. Section III presents and discusses our results for the dipole matrix elements, cross sections, and

angular distributions. In Sec. IV, a summary and conclusions are presented.

II. METHOD OF CALCULATION

If the initial and final states of an alkali-metal atom are expressed as antisymmetric products of single-particle functions, the photoionization cross section for photoionization of the outermost nl subshell is given as¹⁻⁵

$$\sigma_{nl} = \frac{4\pi\alpha a_0^2}{3} (\epsilon - \epsilon_{nl}) \{ l [R_{l-1}(\epsilon)]^2 + (l+1) [R_{l+1}(\epsilon)]^2 \}, \quad (1)$$

where α is the fine-structure constant, a_0 the Bohr radius, ϵ and ϵ_{nl} the photoelectron and binding energies, respectively, in rydbergs, and $R_{l\pm 1}(\epsilon)$ the dipole matrix elements given by

$$R_{l\pm 1}(\epsilon) = \int_0^\infty P_{nl}(r) r P_{\epsilon, l\pm 1}(r) dr, \quad (2)$$

with P_{nl}/r the radial part of the discrete wave function and $P_{\epsilon, l\pm 1}/r$ the radial part of the continuum function. Further details are found elsewhere.¹⁻⁵ These equations take a simple form since, aside from the outermost electron, the alkali-metal atoms consist of only closed shells. In addition, they are the same for excited as well as ground states. Clearly then, a knowledge of the wave functions is tantamount to a knowledge of the dipole matrix elements and the cross sections.

Before going to a discussion of the wave functions, we note that the angular distribution of photoelectron in the dipole approximation (which is excellent for $h\nu < 500$ eV) is given by⁹

$$\frac{d\sigma_{nl}}{d\Omega} = \frac{\sigma_{nl}}{4\pi} [1 + \beta_{nl} P_2(\cos\theta)], \quad (3)$$

where P_2 is a Legendre polynomial, θ is the angle between photon polarization and electron propagation directions, and the asymmetry parameter β_{nl} , is given by¹⁰

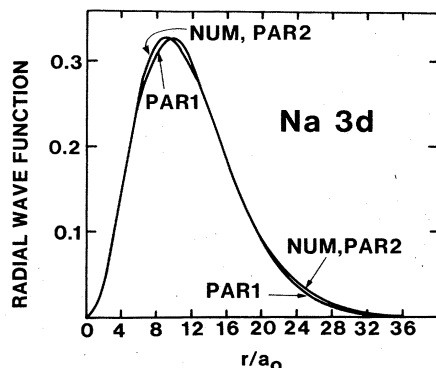


FIG. 1. Radial Hartree-Fock wave function for Na 3d in numerical (NUM) and analytic (PAR1,PAR2) formulations. See text for details.

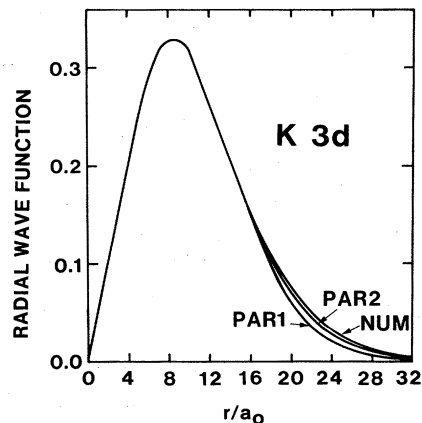


FIG. 2. Radial Hartree-Fock wave function for K 3d in numerical (NUM) and analytic (PAR1,PAR2) formulations. See text for details.

$$\beta_{nl}(\epsilon) = \frac{l(l-1)[R_{l-1}(\epsilon)]^2 + (l+1)(l+2)[R_{l+1}(\epsilon)]^2 - 6(l+1)R_{l-1}(\epsilon)R_{l+1}(\epsilon)\cos(\xi_{l+1} - \xi_{l-1})}{(2l+1)\{l[R_{l-1}(\epsilon)]^2 + (l+1)[R_{l+1}(\epsilon)]^2\}}, \quad (4)$$

with $\xi_{l\pm 1} = \sigma_{l\pm 1} + \delta_{l\pm 1}$, the sum of the Coulomb and non-Coulomb phase shifts.

Two different approaches were used in the generation of the HF wave functions for the initial 3d state. The first¹¹ was a methodology which generated *numerical* wave functions for the initial-state orbitals as well as for those of the ionic core. This is the most accurate method and the resulting wave functions are insensitive to small changes in input parameters. The second¹²⁻¹⁴ was a code which generated *analytic* (parametric) HF wave functions, which are very attractive owing to their simplicity and transportability. This method, however is somewhat sensitive to the input parameters and two different ones were generated. All three wave functions gave the same total and orbital energies, to very high accuracy, and also satisfied the virial theorem extremely well. The numerical wave function shall be referred to as NUM. Of the two types of analytic (parametric) HF wave functions calculated, one was generated with the input parameters adjusted to give a result as close to NUM as possible and is labeled PAR2. The other, obtained without reference to NUM, is designated PAR1. These wave functions are shown in Figs. 1 and 2. It is seen in Fig. 1, for Na, that some small differences in the 3d wave functions are evident near the maximum and in the tail. NUM and PAR2 are identical, to at least the thickness of the lines. For K, seen in Fig. 2, all the functions are virtually identical in the region of the maximum but some differences are evident in the asymptotic region. Note further the spatial extent of these wave functions, more than $30a_0$.

The final (continuum) state HF wave functions were calculated in the core of the positive ion, which is identical in the numerical and analytic approaches (being so compact) using a previously developed code. Details of this calculation are given elsewhere.¹⁵

III. RESULTS AND DISCUSSION

Dipole matrix elements, cross sections, and photoelectron angular distribution asymmetry parameters were calculated for Na 3d and K 3d using each of the initial-state wave functions described in the previous section. Both the length and velocity formulations² of the dipole matrix element were calculated in each case. The final continuum wave functions, however, were invariant to differences in the excited-state wave function as discussed previously.

A. Dipole matrix elements

The dipole matrix elements for the 3d \rightarrow ϵp transition in Na and K, calculated using the three different initial-state wave functions described above, are shown in Figs. 3 and

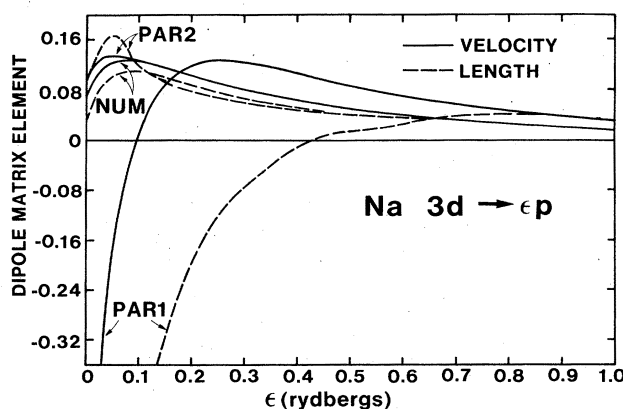


FIG. 3. Dipole matrix element for Na 3d \rightarrow ϵp using three different initial-state wave functions (described in text) in both velocity and length formulations.

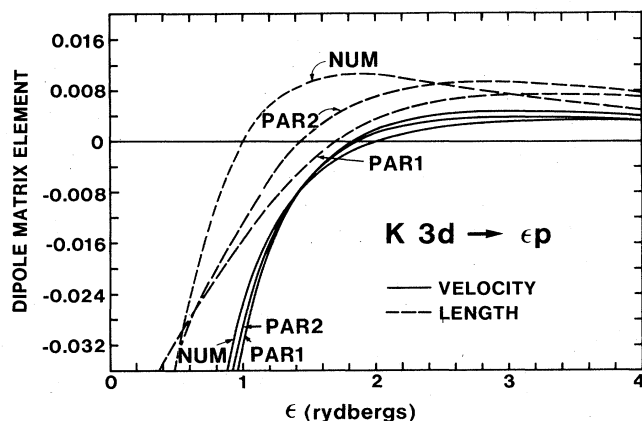


FIG. 4. Dipole matrix element for $K 3d \rightarrow \epsilon p$ using three different initial-state wave functions (described in text) in both velocity and length formulations.

4. For Na, seen in Fig. 3, the calculations based upon slightly different wave functions lead one to opposite conclusions; the dipole matrix elements for PAR2 and NUM show a zero just below threshold, while PAR1 shows the zero in the continuum. It is further remarkable that the PAR2 and NUM wave functions for Na, which when plotted seem to be virtually identical (cf. Fig. 1), give matrix elements which differ near the minimum, in this case in the threshold region. Since the numerical NUM $3d$ wave function is the most accurate solution of the HF equation, this disagreement means that analytic wave functions, no matter how accurate they seem, can lead to difficulties in the neighborhood of a zero in the dipole matrix element. By the same token, away from the minimum region (away from threshold in this case) agreement between NUM and PAR2 is excellent, indicating the utility of analytic wave functions in this region. Furthermore, the PAR1 wave function is only slightly different than the others, but its matrix element is seen to be rather different.

We have used the velocity formulation in arriving at the above observations since the velocity matrix element is far less sensitive to the details of the outer part of the wave function. This outer part of an excited-state discrete wave function is extremely sensitive to the details of the calculation. Thus, the length formulation, which is sensitive to the large- r region, is not particularly trustworthy for excited-state photoionization. As an example, note that the length matrix element for the PAR1 wave function, shown in Fig. 3, also shows a minimum in the continuum but at an energy roughly *five times* the velocity matrix element for PAR1. The length matrix elements for PAR2 and NUM do not show zeros in the continuum and are of the same general shape as the velocity matrix elements but there are some quantitative differences, as much as 20%, and they come together at a much higher energy than the velocity matrix elements. The sensitivity of the dipole length formulation to the wave function employed was previously pointed out in ground-state photoionization,^{15,16} where it was found that larger discrepan-

cies among different approximations occurred in the dipole length formulation. Note has also been made¹⁷ concerning the importance of the asymptotic region in the dipole length formulation in an analysis of oscillator strengths. This effect is magnified for excited states.

Previous calculations of this $Na 3d \rightarrow \epsilon p$ matrix element have been made using simple central-field Hartree-Slater (HS) wave functions.² Actually two different calculations were done, one using the potential appropriate to the excited $3d$ initial state⁷ and one using the potential appropriate to the ground state.¹⁸ Both of these calculations showed a zero in the $d \rightarrow p$ channel, the former at about 0.5 rydbergs and the latter at about 0.1 rydbergs. This further indicates the sensitivity of the $l \rightarrow l-1$ zero to the details of the calculation. We note, in passing, that the HS result based on the ground-state potential is closer to the most accurate HF result than is the other HS calculation.

For the $K 3d \rightarrow \epsilon p$ transition, the results are given in Fig. 4. Note that the energy scale of this plot is about four times that of Fig. 3 for Na. From this figure, it is seen that the $d \rightarrow p$ zero is far enough above threshold that it is predicted to be in the continuum by all three $3d$ wave functions in both length and velocity. Nevertheless, there are significant differences in the positions predicted. The most accurate result, the velocity form of NUM, predicts the zero at just about 2 rydbergs; the PAR1 and PAR2 velocity results give zeros lying close together 1.84 and 1.86 rydbergs, respectively, somewhat below the NUM zero. The length results for these three wave functions are seen to differ considerably, from the velocity results and each other, predicting zeros whose locations differ by as much as 1 rydberg. It is interesting to note that the NUM wave function, the most accurate, gives the largest discrepancy between length and velocity near the zero, but gives the best agreement both well above and well below that region. This indicates the sensitivity of the calculation. The fact that the PAR1 and PAR2 wave functions give better agreement near the zero is considered fortuitous. Finally, we note that both HS results^{7,18} (as described above) predict the zero to be at about 0.3 rydbergs.

Thus, it is seen that the HF calculation moves the zero to lower energies (below threshold) for $Na 3d$, but to higher energies for $K 3d$, as compared with the central-field HS results. This indicates that there is no simple way of judging from a simple HS calculation where the zero will actually be. This matter will be studied further.

We have also calculated, but not shown, the dipole matrix elements for the $3d \rightarrow \epsilon f$ transitions in both Na and K. Here the matrix elements show simple monotone decreases from threshold, with no zeros, and very close to hydrogenic. This is to be expected since the quantum defects of the discrete $3d$ states and the phase shifts of the ϵf continuum states are all close to zero.

B. Cross sections

The total photoionization cross sections for $Na 3d$ and $K 3d$ are shown in Figs. 5 and 6, respectively, for the NUM wave function in both length and velocity. From

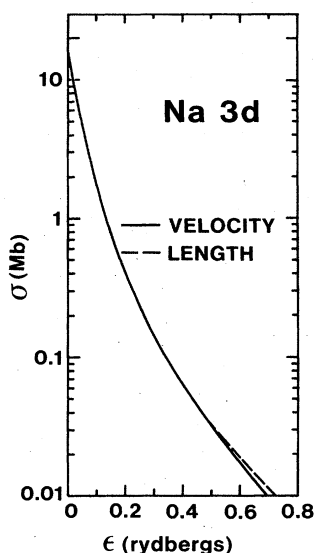


FIG. 5. Total Na $3d$ photoionization cross section using numerical (NUM) initial-state wave functions in both velocity and length formulations.

these results it is clear that the zeros in the $3d \rightarrow \epsilon p$ channels have virtually no effect on the total cross section. This is because the $3d \rightarrow \epsilon f$ channel is the overwhelmingly dominant one in each case. This is hardly surprising since it is usual in atomic photoionization that near threshold, the $l \rightarrow l+1$ channel dominates.^{1,2} Thus the total subshell cross sections cannot be used to determine the location of the $l \rightarrow l-1$ minima, in these cases.

The rather good agreement between length and velocity, seen in Figs. 5 and 6, indicates that HF does a reasonable job on the $3d \rightarrow \epsilon f$ transitions which constitute most of the cross section. The best agreement is near threshold

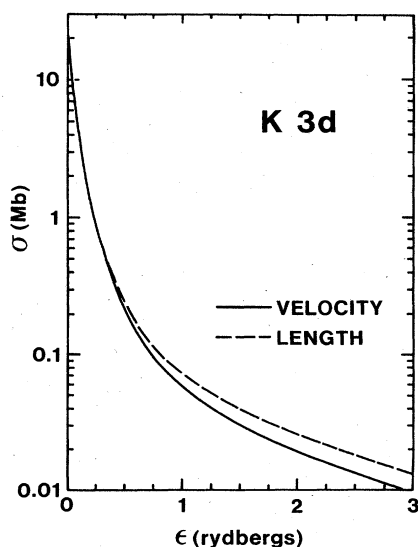


FIG. 6. Total K $3d$ photoionization cross section using numerical (NUM) initial-state wave functions in both velocity and length formulations.

where the ϵf phase shifts are zero and the $3d \rightarrow \epsilon f$ matrix elements are hydrogenic. At higher energies, where the f -wave phase shifts begin to increase,¹⁹ the matrix elements are no longer hydrogenic and small differences between length and velocity start to appear.

C. Photoelectron angular distributions

Although the effects of the $3d \rightarrow \epsilon p$ zeros are unobservable in the total $3d$ cross section, they will be in the angular distribution of photoelectrons, or, more precisely, in the variation of the asymmetry parameter [cf. Eqs. (3) and (4)] with energy. Looking at Eq. (4), it is easy to see that for an initial d state, if there is a zero in the $d \rightarrow p$ channel, $R_{l-1}=0$ and $\beta_{nd}=0.8$. Thus by scrutinizing β , the position of the zero can be inferred.

The asymmetry parameter for Na $3d$ photoionization is shown in Fig. 7 in various approximations. Note that the NUM results, which we believe to be the most accurate, both rise from a threshold value just greater than 0.8, indicating the lack of a zero in the continuum. In fact, extrapolating backwards, we can infer that the zero is just below threshold, just as we concluded from the matrix elements in Fig. 3. Looking at the PAR1 results shown in Fig. 7, it is seen that both length and velocity pass through 0.8 twice. This shows that $\beta=0.8$ is a necessary but not sufficient condition for there to be a $d \rightarrow p$ zero. In fact it is the larger energy at which $\beta=0.8$ in each case that is due to the zero and these occur at precisely the same energies as the zeros predicted by PAR1 as shown in Fig. 3. Thus different shapes of β vs ϵ ensue, depending upon whether there is a zero in the channel.

In Fig. 8, the NUM asymmetry parameter for K $3d$ is shown in length and velocity, both of which pass through 0.8. It is again the second time that $\beta=0.8$ that indicates the $d \rightarrow p$ zero and it is seen that these positions are exactly the same as the location of the NUM zeros for K $3d$ shown in Fig. 4. These results demonstrate that, although the total subshell cross sections are insensitive to the $3d \rightarrow \epsilon p$ zeros, the asymmetry parameters are quite sensitive.

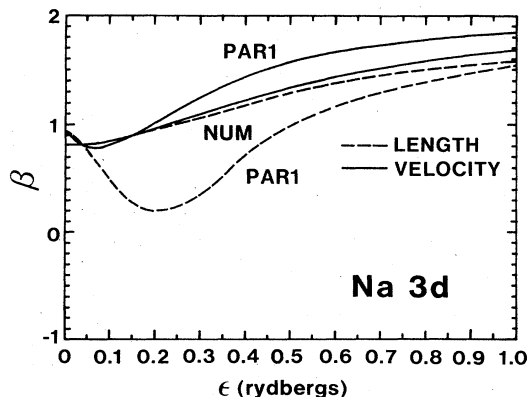


FIG. 7. Photoelectron angular distribution asymmetry parameter β for Na $3d$ in both length and velocity formulations using numerical (NUM) and analytic (PAR1) Hartree-Fock initial-state wave functions.

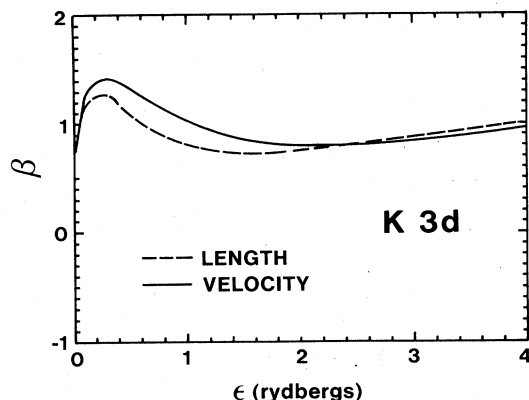


FIG. 8. Photoelectron angular distribution asymmetry parameter β for K 3d in both length and velocity formulations using numerical (NUM) Hartree-Fock initial-state wave functions.

IV. FINAL REMARKS

It has been shown that calculations of dipole matrix elements for Na and K $3d \rightarrow \epsilon p$ photoionizing transitions are *extremely* sensitive to the *initial-state* wave functions in the vicinity of zeros. Analytic HF wave functions, which appeared to be the same as numerical ones, gave rather different predictions for the location of the zeros. It should be noted, in addition, that the initial 3d state has a wave function which is nodeless; the situation is likely to be worse where the initial-state's wave function contains nodes. Thus, extreme caution needs to be taken in the numerical accuracy in excited-state photoionization calculations in the region of minima. The conclusions are also supported in another study.²⁰

It has also been found that the dipole-velocity formulation is much more stable than the dipole-length formulation for reasons discussed above. If there is any reason to suspect the numerical accuracy of the calculation, then, the dipole-velocity matrix element is to be preferred.

The zeros in the $3d \rightarrow \epsilon p$ channel were shown to have

no significant effects on the total 3d photoionization cross section. Their location could, however, be inferred from the behavior of the photoelectron angular distribution asymmetry parameter β as discussed.

At present there is no experimental verification of these zeros in $l \rightarrow l-1$ channels. It would seem that measurements of the asymmetry parameter (which could be accomplished in a relative measurement) would be the best way of looking for these zeros. Since the zeros are not in the dominant $l \rightarrow l+1$ channels, the cross section remains large in the vicinity of the $l \rightarrow l-1$ zeros, thus making laboratory measurements easier. Such measurements are deemed to be quite important to provide a guide to the accuracy of theoretical excited-state photoionization cross sections. The zeros are a particularly good feature to investigate; since they are so sensitive, a calculation which gets them right would almost surely be excellent for total cross sections and angular distributions over a broad energy range.

Although we have no experimental evidence for the cases discussed herein, we can use certain others as a guide. Very good agreement has been found between experiment and a HF calculation using a *numerical* (NUM) initial-state wave function for Cs 6p.²¹ In addition, similarly good agreement with a sophisticated random-phase approximation (RPA) calculation was found for Cs 7p.²¹ These comparisons indicate that correlation effects may not be very significant for excited-state photoionization in the threshold region. Nevertheless, since the $d \rightarrow p$ cross sections are so small a part of the total, correlation could be important in these channels. Thus, although our *numerical* HF calculations place the $d \rightarrow p$ at certain energies (below threshold in the Na 3d case), inclusion of correlation could change these energies significantly.

ACKNOWLEDGMENTS

This work was supported by the U.S. Department of Energy (Office of Basic Energy Sciences) and by the U.S. Army Research Office.

¹U. Fano and J. W. Cooper, Rev. Mod. Phys. **40**, 441 (1968).

²S. T. Manson, Adv. Electron. Electron Phys. **41**, 73 (1976); **44**, 1 (1977).

³A. F. Starace, in *Handbuch der Physik*, edited by W. Mehlhorn (Springer-Verlag, Berlin, 1982), Vol. 31, p. 1.

⁴J. W. Cooper, Phys. Rev. **128**, 681 (1962).

⁵S. T. Manson and J. W. Cooper, Phys. Rev. **165**, 126 (1968).

⁶A. Msezane and S. T. Manson, Phys. Rev. Lett. **35**, 364 (1975).

⁷A. Msezane and S. T. Manson, Phys. Rev. Lett. **48**, 473 (1982).

⁸N. B. Avdonina and M. Ya. Amusia, J. Phys. B **16**, L543 (1983).

⁹C. N. Yang, Phys. Rev. **74**, 764 (1948).

¹⁰J. Cooper and R. N. Zare, in *Lectures in Theoretical Physics*, edited by S. Geltman, K. Mahathappa, and W. Britten (Gordon and Breach, New York, 1969), Vol. 11c, pp. 317–337.

¹¹C. Froese Fischer, Comput. Phys. Commun. **4**, 107 (1972).

¹²C. J. Roothan and P. S. Bagus, Methods Comput. Phys. **2**, 47

(1963).

¹³B. Roos, C. Salez, A. Veillard, and E. Clementi, IBM Technical Report RJ518, 1968 (unpublished).

¹⁴E. Clementi and C. Roetti, At. Data Nucl. Data Tables **14**, 177 (1974).

¹⁵D. J. Kennedy and S. T. Manson, Phys. Rev. A **5**, 227 (1972).

¹⁶M. J. Seaton, Proc. R. Soc., Ser. A **208**, 418 (1951).

¹⁷A. Burgess and M. Seaton, Mon. Not. R. Astron. Soc. **120**, 9 (1960).

¹⁸J. Lahiri and S. T. Manson, *Abstracts of Papers of the Twelfth International Conference on the Physics of Electronic and Atomic Collisions, Gatlinburg, Tenn., 1981*, edited by S. Datz (North-Holland, Amsterdam, 1982), p. 39.

¹⁹S. T. Manson, Phys. Rev. **182**, 97 (1969).

²⁰A. Z. Msezane, Phys. Rev. A **29**, 3431 (1984).

²¹A. Z. Msezane, J. Phys. B **16**, L489 (1983).